I&EC research
Industrial & Engineering Chemistry Research

Article

pubs.acs.org/IECR

Polymerization and Functionalization of Membrane Pores for Water Related Applications

Li Xiao,[†] Douglas M. Davenport,[†] Lindell Ormsbee,[‡] and Dibakar Bhattacharyya*,[†]

[†]Department of Chemical and Materials Engineering and [‡]Department of Civil Engineering, University of Kentucky, Lexington, Kentucky 40506, United States

ABSTRACT: Poly(vinylidene fluoride) (PVDF) was modified by chemical treatments in order to create active double bonds to obtain covalent grafting of poly(acrylic acid) (PAA) on membrane. The attenuated total reflectance Fourier transform infrared (ATR-FTIR) spectrum confirms the formation of conjugated C═C double bonds with surface dehydrofluorination. The membrane morphology was studied by scanning electron microscopy (SEM). The surface composition was characterized by X-ray photoelectron spectroscopy (XPS). The thermal stability of the dehydrofluorinated membrane (Def-PVDF) and functionalized membranes were investigated by differential scanning calorimetry (DSC) analysis. The influence of covalently attached PAA on Def-PVDF membrane has been investigated to determine its effect on the transport of water and charged solute. Variations in the solution pH show an effect on both permeability and solute retention in a reversible fashion. Metal nanoparticles were also immobilized in the membrane for the degradation of toxic chlorinated organics from water. In addition, PVDF membranes with an asymmetric and sponge-like morphology were developed by immersion-precipitation phase-inversion methods in both lab-scale and large-scale. The new type of spongy PVDF membrane shows high surface area with higher yield of PAA functionalization. The ion-capacity with Ca^{2+} ions was also investigated.

1. INTRODUCTION

Poly(vinylidene fluoride) (PVDF) is a widely studied and used polymer, especially for industrial application due to its excellent chemical, mechanical, and UV stability properties.[1−3] PVDF membranes have been extensively used in ultrafiltration (UF) and microfiltration (MF) applications for separation processes and wastewater treatment and currently are explored as contactors and in bioseparation applications.[1,2,4−7] An interesting new application is involving the use of PVDF blends to make artificial muscles.[8] In addition, there is increasing interest in the modification of PVDF membranes with environmentally sensitive functionalities for many diverse applications such as drug delivery, cell encapsulation, electronic devices, sensors, and water softening.[9−13]

To meet the needs of the desired application, PVDF membranes can be chemically and/or physically modified. Various methods are currently used such as coating,[14] adsorption,[15] the grafting of functional groups or graft polymerization to the membranes,[2,16−18] and chemical modification of membrane materials.[19] In our previous work, we described methods for obtaining PVDF membranes with pH and temperature responsive properties via in situ hydrogel cross-linking or in situ polymerization in solvent phase.[11,20,21] These functionalized membranes were subsequently used as a support to immobilize Fe or Fe/Pd nanoparticles to remove toxic chloro-organics from groundwater.[21,22] In this work, we extend previous studies and present a new method to form covalently attached polymers onto the PVDF membranes involving chemical treatment of the pristine membrane with alkaline solutions to obtain dehydrofluorinated PVDF membranes. The reaction mechanism of alkaline degradation of PVDF is shown as follows:[23−27]

$$—(CH_2—CF_2)— + XOH \rightarrow —(CH═CF)— + XF + H_2O$$

where X = Na, K, or Li.

The dehydrofluorinated PVDF polymer forms conjugated double bonds or a polyene structure which can be attacked by specific reactants to introduce functional groups to the membrane, such as acrylic acid (AA). The introduction of covalent bonding can eliminate the concerns on the stability of poly(acrylic acid) chains on the PVDF membrane prepared by the in situ hydrogel cross-linking method.

As mentioned above, the PVDF membrane support is further used to immobilize metal nanoparticles for a dechlorination reaction. As expected, a higher metal loading leads to a higher reaction rate, and a higher surface area of the support PVDF membrane is required to achieve a greater degree of metal loading. Therefore, in this work, another improvement was achieved through the modification of pristine PVDF structure. PVDF membranes are usually made by a phase inversion method induced by immersion of a cast solution in a polymer nonsolvent bath.[28,29] The membrane morphology, porosity, flux and retention properties can be altered by changing the casting and immersion parameters.[1,30,31] In this work, a sponge-like PVDF membrane is designed to have higher ion adsorption capacity which results in higher nanoparticle loading.

The dehydrofluorination of PVDF membranes has been reported. However, the application of dehydrofluorinated

Special Issue: Scott Fogler Festschrift

Received: October 20, 2014
Revised: December 15, 2014
Accepted: December 15, 2014
Published: December 15, 2014

DOI: 10.1021/ie504149t
Ind. Eng. Chem. Res. 2015, 54, 4174−4182

PVDF for covalent attachment of different polymers for reaction and separation has been reported very little.[2,4] The main goals of the present study are to (1) create dehydrofluorinated membranes for the introduction of proper functional groups through covalent bonding; (2) investigate the effect of alkaline treatment time on the membrane structure; (3) study the pH responsive behavior of functionalized PVDF membranes; and (4) prepare sponge-like PVDF membranes with high surface area and metal loading.

2. EXPERIMENTAL SECTION

2.1. Materials. Full-scale pristine PVDF membranes were obtained from Ultura Inc. Oceanside, CA. Sodium hydroxide (NaOH), acrylic acid (AA), ammonium persulfate (APS), ferrous chloride tetrahydrate ($FeCl_2 \cdot 4H_2O$), sodium borohydride ($NaBH_4$), trichloroethylene (TCE), *N*,*N*-dimethylfomamide (DMF), and lithium chloride (LiCl) were purchased from Sigma-Aldrich. Deionized ultrafiltered water (DIUF) was purchased from Fisher Scientific. The PVDF powder was a commercial product (Kynar 761) (M_w = 350 000 g/mol) kindly offered by Ultura Inc. Oceanside, CA. Polyvinylpyrrolidone (PVP) (M_w = 40 000 g/mol) was purchased from Polysciencs, Inc. Ultrahigh purity (UHP) nitrogen gas used in flux experiments was purchased from Scott Specialty Gases. All chemicals were used without further purification.

2.2. Dehydrofluorination of PVDF Membrane (Def-PVDF). A piece of PVDF membrane was soaked in 15 wt % NaOH solution in 40 mL DIUF for 10 min. Then, the membrane was sandwiched between two glass plates and placed in an oven at 70 °C to react for 1, 3, and 22 h. The final membrane was washed with DIUF until the pH became neutral.

2.3. PAA Functionalization of PVDF Membranes (PAA-Def-PVDF) by Pore-Filling. The dehydrofluorinated PVDF membrane was functionalized with PAA by in situ polymerization with acrylic acid. The polymerization reaction was performed in an aqueous solution. The polymerization solution contained 11.1 wt % acrylic acid (monomer) and 0.4 wt % of APS (initiator). The Def-PVDF membrane was dipped in the polymerization solution for 5 min, sandwiched between two glass plates, and placed in an oven at 90 °C for 2 h. The undehydrofluorinated PVDF membrane was also functionalized with PAA as a control by using the same pore-filling method.

2.4. Preparation of Spongy PVDF Membranes (SPVDF). The spongy PVDF membranes were made using the phase inversion method. The casting solution was made of 20 wt % PVDF, 2 wt % PVP, 2.25 wt % LiCl, and 75.75 wt % DMF and heated to 50 °C. A film of PVDF solution was first cast on a glass plate (23−25% humidity) and then immersed in DIUF water at 50 °C for coagulation. After 10 s, the formed membrane was put in pure DIUF water at 23 °C to wash and let it dried in an oven at 70 °C. The full-scale SPVDF was also fabricated under the same conditions by Ultura Inc. Oceanside, CA, to assess the feasibility of continuous membrane production. The thickness of membrane was 175 μm.

2.5. Attenuated Total Reflectance Fourier Transform Infrared Spectroscopy (ATR-FTIR). Attenuated total reflectance Fourier transform infrared (ATR-FTIR) spectroscopy (Varian 7000e) was used to determine the presence of functional groups in dehydrofluorinated PVDF and functional membranes. The samples were placed on the diamond crystal, and the spectrum was obtained between 500 and 4000 cm^{-1} for 32 scans at a resolution of 8 cm^{-1}.

2.6. Scanning Electron Microscopy (SEM). The surface and cross-section morphology of the blank PVDF, Def-PVDF, functionalized membranes, and spongy PVDF were studied using a Hitachi S-4300 scanning electron microscope (SEM). The samples were mounted on sample studs, and a thin layer of gold was sputtered on the sample surface for imaging purpose. The SEM measurements were performed at an accelerating voltage of either 10 or 3 kV.

2.7. X-ray Photoelectron Spectroscopy (XPS) Analysis of Membrane Surface. The surface composition of membrane was characterized using an X-ray photoelectron spectroscopy (Thermo Scienctific K-Alpha) with Al/K ($h\gamma$ = 1486.6 eV) anode mono X-ray source. The sample was directly mounted on a sample holder then transferred into the analyzer chamber. The entire spectra of all the elements were recorded with very high resolution using Avantage software. Each survey spectra was the average of five survey scans.

2.8. Water Flux Measurement. The water permeability was measured at different pH levels to study the pH responsive flux behavior of PAA-Def-PVDF. The tested membrane was mounted in a stirred cell (Millipore) which contains feedwater of varying pH. The cell was pressurized at different pressures using pure nitrogen. Once the membrane flux reached steady-state, volume flux was measured in triplicates by recording the volume passed through the membrane in a given time interval. The final test was conducted at pH 4 to test for reversibility.

2.9. Na_2SO_4 Rejection. Na_2SO_4 rejection experiments were performed using a stirred membrane cell provided by Millipore with a membrane cross-sectional area of 13.2 cm^2 which included a stirring device to minimize the effects of concentration polarization. The feed Na_2SO_4 concentration was 100 mg/L. The permeate sodium concentration was measured with a Varian AA220 series atomic absorption spectrophotometer.

2.10. Synthesis of Fe/Pd Nanoparticles in Membrane and Dechlorination. The method for the synthesis of nanoparticles was developed by our group and described previously.[32−34] The Fe/Pd nanoparticles were made by an ion-exchange with Fe^{2+}, the reduction with sodium borohydride, and a post-palladium coating. The dechlorination was conducted in a 40 mL vial loaded with nanoparticles and fed a TCE solution at 30 mg/L. The TCE concentration was determined after a certain time interval by extracting the sample with pentane and analyzing by gas chromatography (HP Series II model 58590) with a mass spectrometer (GC-MS). Detailed information about nanoparticles synthesis and dechlorination can be found elsewhere.[11,20,32]

3. RESULTS AND DISCUSSION

3.1. Dehydrofluorination and PAA Functionalization of PVDF Membranes. The PVDF membranes were treated with 15 wt % of sodium hydroxide for different treatment times. Prior to the treatment, the PVDF membranes were white in appearance. After treatment, a color change was observed for all the membranes from white to a light yellow or deep yellow or even black as shown in Figure 1. The ATR-FTIR spectra of blank PVDF, Def-PVDF, and PAA-Def-PVDF membranes are shown in Figure 2. The characteristic peaks at 1403 and 1600 cm^{-1} are corresponding to —CH_2 and C═C, respectively (Figure 2B−D). This is due to the formation of polyene in the membrane as the fluorocarbon groups of PVDF are changed by the treatment (1000−1250 cm^{-1}) (Figure 2A). As the treatment time is increased, the intensity of the carbon double

DOI: 10.1021/ie504149t
Ind. Eng. Chem. Res. 2015, 54, 4174−4182

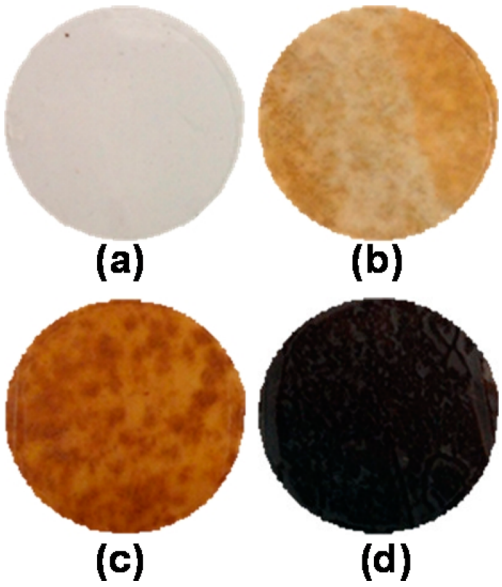

Figure 1. Change in color of the PVDF membranes after treatment with 15 wt % of NaOH for different hours at 70 °C: (a) 0, (b) 1, (c) 3, (d) 22 h.

bond response increases. It should be noted that the low absorbance intensity at 1600 cm^{-1} is due to the inactive C═C bond in infrared.[23] The hydrocarbon at peaks 1350−1450 and 800−900 cm^{-1} do not change significantly with treatment.

As for the PAA functionalized Def-PVDF membranes, the appearance of an obvious peak at 1720 cm^{-1} belongs to the −COOH stretching vibration. To prove the covalent attachment of PAA with Def-PVDF, no cross-linker was used for the PAA functionalization. After several washes with DIUF, the hydrophilic PAA was not washed out. This result together with the ATR-FTIR spectra obviously demonstrates that the PAA was successfully covalently grafted onto the surface of the PVDF membrane.

3.2. SEM Analysis. The morphologies of the blank and functionalized PVDF membranes were characterized by SEM as shown in Figure 3. A pristine PVDF membrane (Figure 3a) shows fairly porous structure with mostly circular shape and uniform pore size. The effect of treatment time with NaOH on the structure of membrane was also investigated by SEM, and the results can be seen in Figure 3b and c. When treated for a short amount of time (such as 1 or 3 h), no change in the membrane surface was observed as shown in Figure 3b. On the other hand, large pores are formed on the membrane surface (Figure 3c) after being treated for 22 h. It was also found that the membrane was easy to crack with less mechanical force due to the loss of fluorine by the dehydrofluorination treatment. Additionally, from Figure 3d, it can be clearly seen that PAA is grafted on the membrane surface and also has little effect on the structure of the PVDF membrane.

3.3. XPS Analysis of PAA-PVDF Membranes. The surface compositions of the blank membrane, Def-PVDF, and PAA-Def-PVDF membranes were investigated by XPS. Figure 4 shows the respective survey spectra of these membranes. Compared with a blank PVDF membrane (Figure 4a), the dehydrofluorinated PVDF membrane (Figure 4b) shows a higher level of noise due to the change in surface roughness after treatment with NaOH solution. The dehydrofluorination is proved by a reduction of fluorine intensity, and relative increase of carbon intensity. The decrease in fluorine

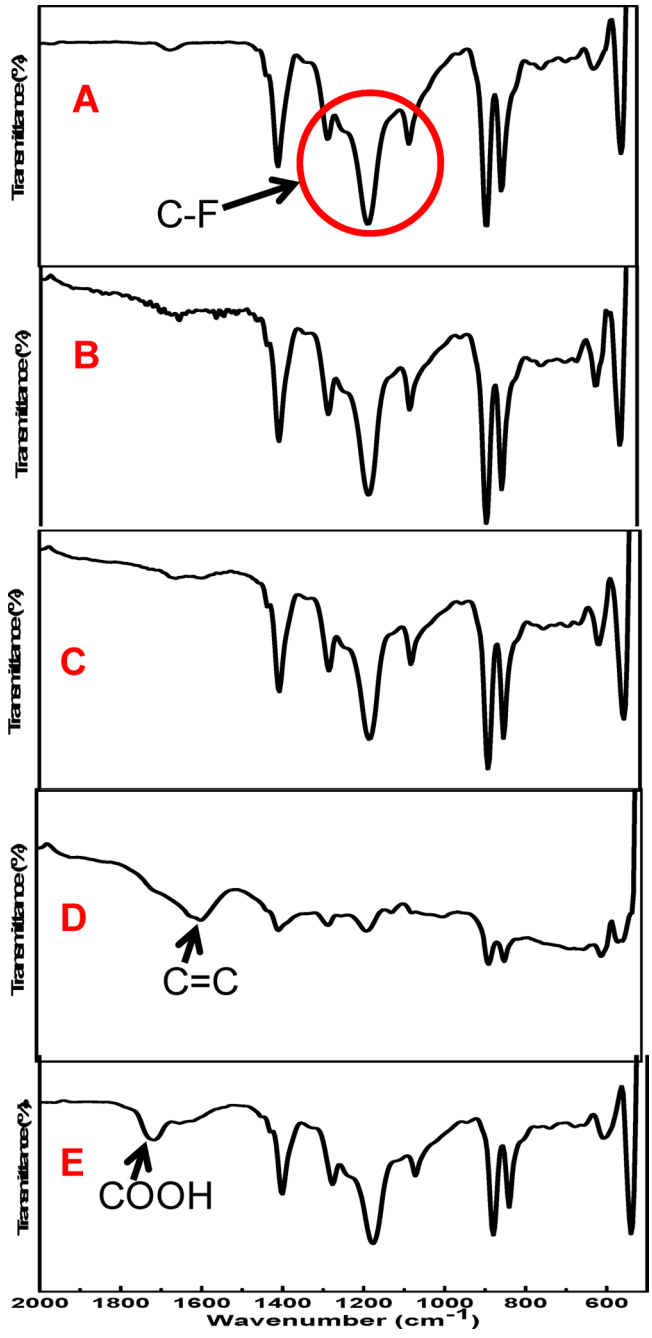

Figure 2. ATR-FTIR spectrum of blank PVDF, Def-PVDF, and PAA-Def-PVDF membranes. (A) Blank PVDF; (B) Def-PVDF with 1 h NaOH treatment; (C) Def-PVDF with 3 h NaOH treatment; (D) Def-PVDF with 22 h NaOH treatment; (E) PAA-Def-PVDF (PAA functionalization of sample C). The percentage of transmission scales is varied in the range 100−40%.

concentration and the increase in carbon concentration with time are also shown in Figure 5, which indicate that most of the dehydrofluorination happens in the first hour of the treatment, and it is also seen that the rate of reaction slows down as treatment time increases. As shown in Figure 4c, the increase of carbon and oxygen intensity indicates that the PAA was grafted on the membranes. Figure 6 show the respective C 1s core-level spectra of the blank PVDF (Figure 6a) and PAA-Def-PVDF (Figure 6b) membranes. The blank PVDF membrane can be fitted with two main peaks at 286 eV for CH_2 groups and 290.6

DOI: 10.1021/ie504149t
Ind. Eng. Chem. Res. 2015, 54, 4174−4182

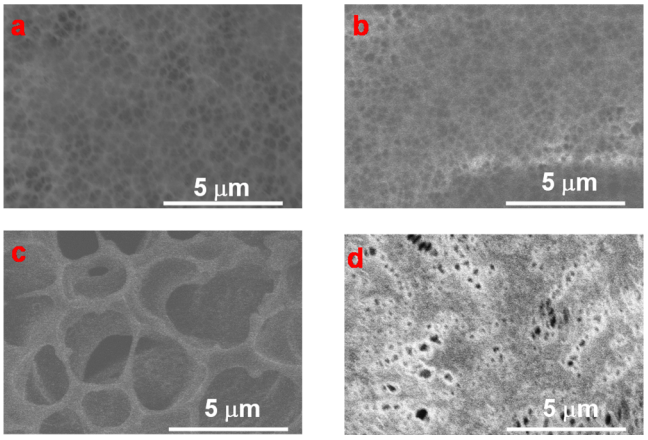

Figure 3. SEM image of blank PVDF (a: sample A in Figure 2), dehydrofluorinated PVDF-3h (b: sample C in Figure 2) and -22h (c: sample D in Figure 2), and PAA-Def-PVDF (d: sample E in Figure 2).

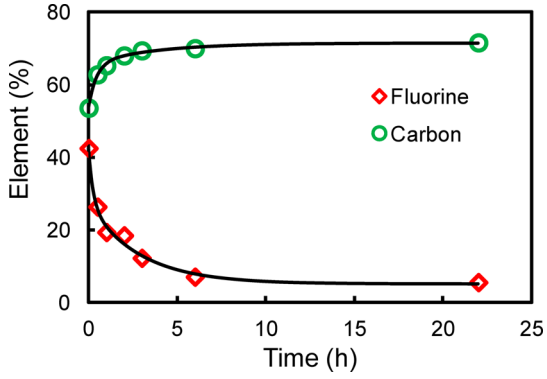

Figure 5. Changes in XPS elemental percentages of fluorine and carbon with different treatment time using15 wt % NaOH.

eV for CF_2 groups.[11,23] On the other hand, the C 1s spectra of the PAA-Def-PVDF membrane can be fitted with five chemical species. The peak with binding energy of 288.5 eV belongs to the C═O species of the grafted acrylic acid (AA) groups.[11] The peak with binding energy at 286.4 eV can be assigned to C−O of AA groups and the peak with binding energy at 284.6 eV is assigned to CH_2 groups from the grafted PAA polymer.[35]

3.4. Thermal Analysis of the Membranes. Figure 7 shows the DSC curves of the pristine PVDF, Def-PVDF, and PAA-Def-PVDF membranes. It is well-known that pristine PVDF membrane is a partially crystalline polymer because of its symmetrical structure and a melting point of about 173 °C.[18] After dehydrofluorination, the melting point for the Def-PVDF membrane does not change as seen in Figure 7b. However, after the covalent binding of PAA on the dehydrofluorinated PVDF membranes, the symmetrical structure of the pristine PVDF is partially destroyed resulting in the decrease of the melting point to 168 °C (Figure 7d). On the other hand, the PVDF membranes functionalized with PAA by pore-filling methods show no obvious change in the melting point (Figure 7c) due to the formation of polymer blends. Thus, the DSC results suggest that the grafting of PAA chains on the pristine PVDF membrane structure should impart the membranes with enhanced and stable functionalities.

3.5. pH Responsive Permeability of PAA-Def-PVDF. Since PAA was present in the functionalized membranes, a response of water permeation through the membrane with pH

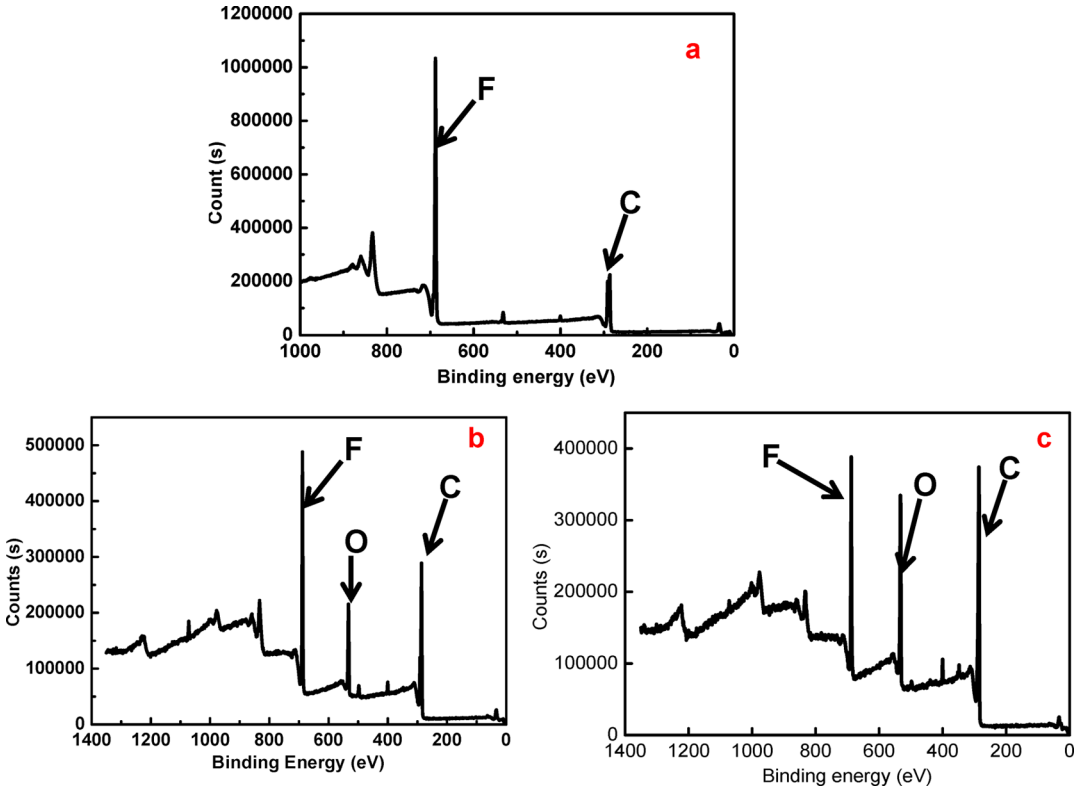

Figure 4. XPS survey spectra of PVDF (a: sample A in Figure 2), Def-PVDF (b: sample C in Figure 2), and PAA-Def-PVDF (c: sample E in Figure 2).

DOI: 10.1021/ie504149t
Ind. Eng. Chem. Res. 2015, 54, 4174−4182

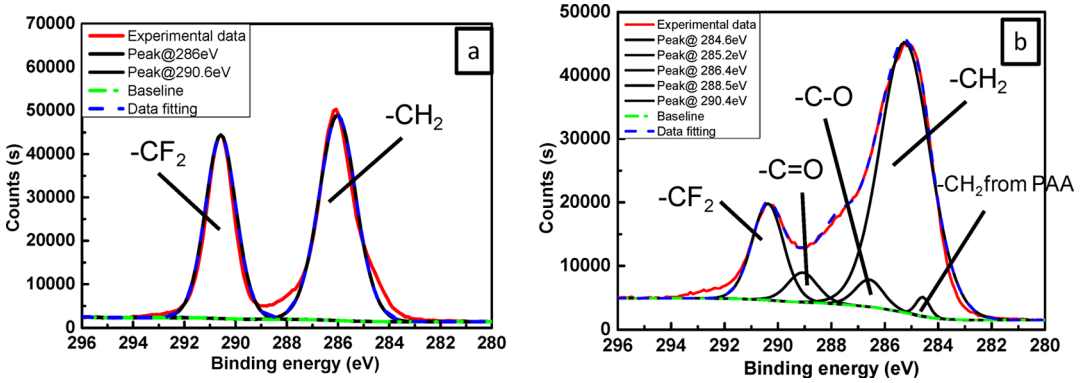

Figure 6. XPS C 1s core-level spectra of pristine PVDF (a: sample A in Figure 2) and PAA-Def-PVDF (b: sample E in Figure 2) membranes.

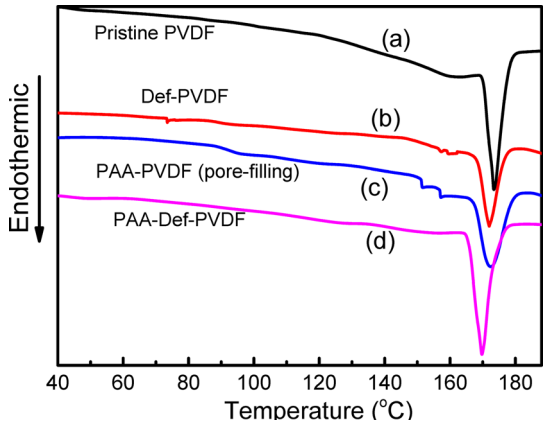

Figure 7. DSC thermogram of (a) pristine PVDF (sample A in Figure 2), (b) Def-PVDF (sample C in Figure 2), (c) PAA-PVDF by the pore-filling method, and (d) PAA-Def-PVDF (sample E in Figure 2).

would be expected. The pH effect on the water permeability of PAA-Def-PVDF functionalized membranes is shown in Figure 8. For comparison, the permeability of a pristine PVDF

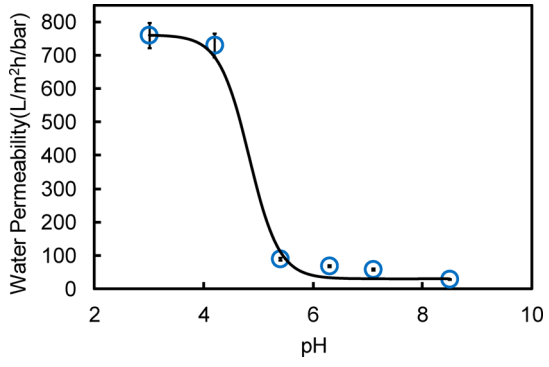

Figure 8. pH effect on the pure water permeability of the PAA-Def-PVDF functionalized membrane.

membrane and Def-PVDF membrane are 964 and 1474 L/m^2·h·bar, respectively. As expected, when the membrane was functionalized with PAA, the flux decreases due to the filling of pores with PAA polymer. It is also seen that as the pH of the feed solution increases, the water flux decreases. This is consistent with previous findings where similar tests were done with PAA functionalized PVDF membrane by the pore-filling method.[32] The change in flux as a response to the change in pH can be caused by the conformational change of acrylic acid polymer chains in the membrane. The linear relationship between water flux and applied pressure resulting in constant flux at pH 4 for different experimental runs indicate that the PAA functionalization on the membrane is very stable. The water permeability data can be fitted with the following equations[36] to obtain the pK_a:

$$L_P = \left(L_{P,max}^{1/2} - \frac{[COO^-]}{[COOH] + [COO^-]}\left(L_{P,max}^{1/2} - L_{P,min}^{1/2}\right)\right)^2 \quad (1)$$

$$\frac{[COO^-]}{[COOH] + [COO^-]} = \frac{1}{1 + 10^{pK_a - pH}} \quad (2)$$

where, $L_{P,max}$ and $L_{P,min}$ are the maximum permeability (760 L/m^2·h·bar) and minimum permeability (29.1 L/m^2·h·bar) when the pH is increased from 3 to 8.5. The experimental data were fitted with both equations and the pK_a was found to be 5.2, which is consistent with the literature reported pK_a value for PAA.[36,37]

3.6. Ca $^{2+}$ Pickup. The amount of −COOH groups in the functionalized membrane was characterized by the amount of Ca^{2+} entrapped by the membrane due to the high affinity of the free −COOH groups to Ca^{2+}. To do this, 100 mL of a 1000 mg/L Ca^{2+} solution was permeated through the membrane to investigate the loading capacity of Ca^{2+}. The feed and permeate samples were collected, and the Ca^{2+} concentrations were analyzed using a Varian AA220 series atomic absorption spectrophotometer. The amount of Ca^{2+} pickup is 0.015 mmol/cm^2 membrane area. Based on ion exchange principles, the assumption is that 1 mol Ca^{2+} can be bound to 2 mol carboxyl groups. Therefore, the calculated −COOH quantity is 0.03 mmol/cm^2. Our previous publication[32] showed that for PAA-PVDF membranes functionalized by pore-filling methods, Ca^{2+} pick-up can range from 0.008 to 0.014 mmol/cm^2 for different degrees of cross-linking. Here, the proper amount of cross-linker is required to keep the PAA functionalization stable without washing out. On the other hand, it has been found that too much cross-linking will block membrane pores and increase the mass transfer resistance. The covalent binding of PAA onto the membrane surface offers a solution to avoid this problem.

3.7. Na_2SO_4 Rejection. The effect of pH on the ion exclusion of the PAA functionalized Def-PVDF membrane is evaluated, and the results are shown in Figure 9. With a pH of 8, the average solute rejection is about 70%. Meanwhile at lower pH (around pH 4), the observed rejection is decreased to

DOI: 10.1021/ie504149t
Ind. Eng. Chem. Res. 2015, 54, 4174−4182

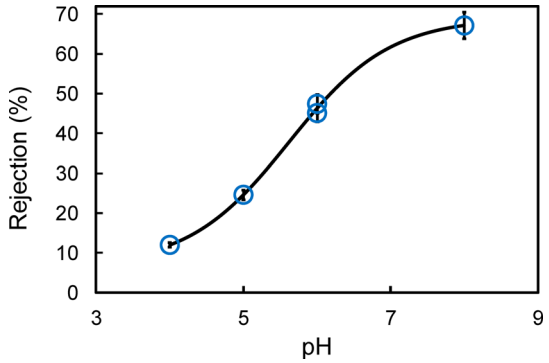

Figure 9. Effect of feed solution pH on the ion exclusion (P = 0.7 bar) of a 100 mg/L Na_2SO4 solution through PAA-Def-PVDF membrane.

10%. This dramatic decrease of solute rejection is because of the helix−coil transitions of the PAA chain in response to the pH change.[38,39] At lower pH, the PAA chain is protonated, which can reduce the overall charge and thus decrease the electrostatic interaction between the membrane and permeate ions.[40] When the pH increases to pH 8, the PAA is ionized with enhanced electrostatic interaction and thus a higher rejection is seen.

The relationship between Na_2SO_4 rejection and permeate flux for a PAA functionalized PVDF membrane is shown in Figure 10. The inset figure shows the linear relationship

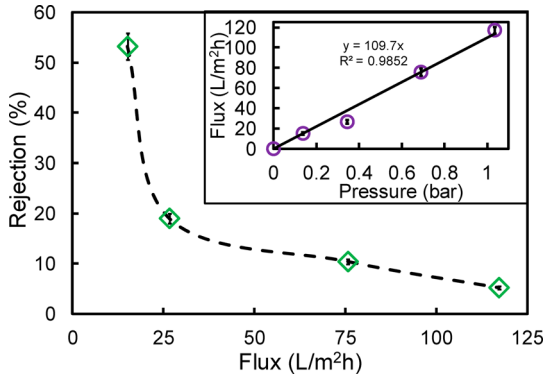

Figure 10. Effect of operating pressures on the ion exclusion of a 100 mg/L Na_2SO4 solution at pH = 6.5. The inset is the water flux (pH = 6.5) dependence on pressure.

between the pressure and flux, which indicates the absence of membrane fouling. The observed decline in rejection at a higher flux is in direct contrast to experimental trends generally observed for ion separations in dense media such as reverse osmosis (RO) and nanofiltration (NF). For NF type membranes, it is seen that the solution rejection increases with increasing flux due to the reduced effect of diffusion. The microporous membranes used in this study show a nonuniform distribution within the pore geometry. This is primarily due to the incomplete pore coverage resulting from nonuniform functionalization or a low chain length to pore ratio. At higher applied pressures, there is enhanced flow through the region of the membrane that is not covered by PAA chains due to the reduction in hydrodynamic thickness of the PAA layer.[41] Commercial nanofiltration membranes are reported to have a 95 to 99% Na_2SO_4 rejection. However, these membranes have a pore size of about 1 nm and are operated at pressures ranging from 10 to 40 bar.[42,43] This specific experiment involves pressure of only about 0.7 bar. Therefore, the development of much more effective membranes will require much higher PAA loading and the limitation of the core region.

3.8. Reductive Dechlorination. Nanoparticles were used for the dechlorination of trichloroethylene (TCE), a ubiquitous pollutant in groundwater. Figure 11 shows the successful

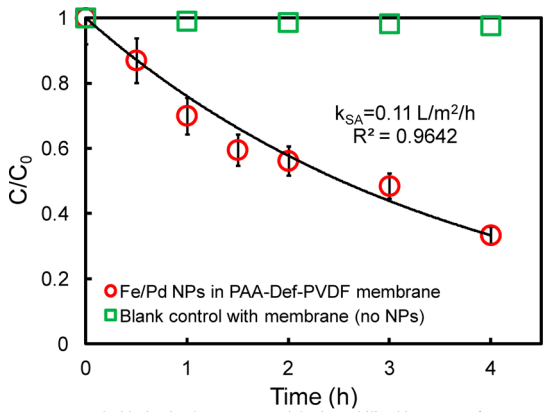

Figure 11. TCE dechlorination by Fe nanoparticles immobilized in PAA-Def-PVDF membrane: vol = 43 mL, initial pH = 6.8, initial TCE concentration = 30 mg/L, iron loading amount = 0.2 g/L (Pd = 1.4 wt % of Fe), temperature = 25 °C.

degradation of TCE with time by Fe/Pd nanoparticles. This reaction can be modeled as a pseudo-first-order heterogeneous reaction:[44−46]

$$\frac{dC}{dt} = -k_{SA}\alpha_s\rho_m C \tag{3}$$

where C is the TCE concentration in water (mg/L); k_{SA} is the surface area normalized reactivity (L/m²·h); α_s is the specific surface area of nanoparticles (m²/g); ρ_m is the mass concentration of nanoparticles (g/L), and t is the time (h). Under the reaction conditions leading to the results in Figure 11, k_{SA} is calculated to be 0.11 L/m²·h which is consistent with the literature reported dechlorination reactivity by Fe/Pd nanoparticles.[33,47−49]

3.9. Spongy PVDF Membranes (SPVDF). As discussed in previous session, the effective dechlorination or ion separation require high loading of PAA into the membrane pores. Therefore, spongy PVDF membranes were first prepared by the phase-inversion method in lab-scale. The full-scale SPVDF was later developed to assess the feasibility of continuously manufacturing these membranes. Both membranes show the same water permeability. In this study, full-scale SPVDF was used to enhance the membrane uniformity and stability. The morphologies of spongy PVDF membranes are shown in Figure 12. It is clearly seen that the overall structure of the membrane cross-section is asymmetrical consisting of a skin surface (Figure 12a) on the top layer supported by a macroporous spongelike sublayer (Figure 12b−d). These macrovoids became more accentuated and extended throughout the entire cross-section. The void volume of the spongelike PVDF membrane can be estimated as follows:[50]

$$\text{void volume (\%)} = [(V_m - V_p)/V_m] \times 100 = \frac{LA - (W_m/\rho_p)}{LA} \times 100 \tag{4}$$

DOI: 10.1021/ie504149t
Ind. Eng. Chem. Res. 2015, 54, 4174−4182

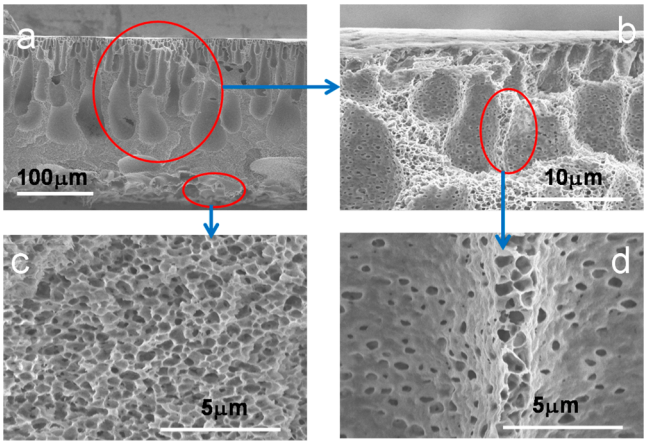

Figure 12. SEM images of cross-section spongy PVDF morphology under different magnification: (a) whole picture, ×300; (b) skin surface and macroporous matrix, ×4000; (c) interconnected fibrous structure in the microporous matrix, ×10 000; (d) microporous matrix under skin surface, ×10 000.

where V_m and V_p are the membrane volume and volume occupied by PVDF polymer respectively, L is the PVDF membrane thickness (cm), A is the membrane area (cm^2), W_m is the membrane mass (g), and ρ_p is the density of PVDF (about 1.78 g/cm^3). The properties of the SPVDF membranes were compared with our previous PVDF membranes from Millipore as shown in Table 1. The SPVDF membrane shows

Table 1. Comparison of SPVDF and PVDF (Millipore)

membrane	PVDF layer thickness (μm)	porosity	BET surface area (m^2/g)	permeability ($L/m^2 \cdot h \cdot bar$)
SPVDF	175	78.6%	7.7	32
PVDF(Millipore)	125[a]	70%	2.1	4400[b]

[a]Supplied by manufacturer. [b]Smuleac et al.[32]

high porosity at about 78.6% and almost 4 times higher surface area compared with that of PVDF (Millipore). Although the SPVDF showed less permeability, the skin layer can enhance antifouling properties due to the prevention of large particles deposition into membrane pores. While the highly porous structure below the skin layer without tortuosity can reduce the residence time of solute and eliminate the mass transfer resistance.[50]

With more surface area, a higher grafting yield will be expected. Therefore, these two membranes were functionalized with acrylic acid under the same conditions, and the results are shown in Table 2. As expected, the SPVDF shows high grating yield at about 81.1 wt % compared to 13% for PVDF (Millipore). The ion exchange capacity was evaluated by Ca^{2+} pickup on these two functionalized membranes. The adsorption capacity of the PAA-SPVDF increases in the first hour and then remains relatively constant at 3.2 mg/cm^2 (265.1 mg/g). The PAA-SPVDF membrane shows high ion-exchange performance with an adsorption capacity that is 10 times higher than PAA-PVDF (Millipore) as shown in Table 2. The SEM-EDS spectra shows the elemental composition and distribution of species and gives the atom ratio of 3.3 (oxygen per calcium) (Figure 13). This value agrees well with the established PAA-metal binding stability constant.[51]

Table 2. Comparison of PAA Functionalization of SPVDF and PVDF (Millipore)[a]

membrane	weight gain (%)[b]	permeability ($L/m^2 \cdot h \cdot bar$)	adsorption capacity (mg Ca^{2+}/cm^2)	adsorption capacity (mg Ca^{2+}/g membrane)[c]
PAA-SPVDF	81.1	5.8	3.2	265.1
PAA-PVDF (Millipore)[d]	13	23	0.32	14.4

[a]Adsorption data obtained using 1000 mg/L $CaCl_2$ solution at pH 6.3. [b]Weight gain from acrylic acid functionalization in pores. [c]"g membrane" refers to total weight without support fabric. [d]Smuleac et al.[32]

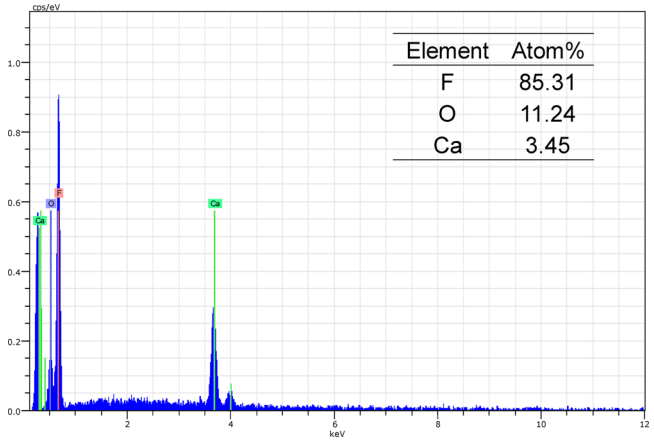

Figure 13. SEM-EDS spectra of PAA-SPVDF membranes loaded with calcium ions.

4. CONCLUSION

The PVDF membrane treated with alkaline solution leads to a modified membrane (Def-PVDF) with conjugated double bonds which were confirmed by ATR-FTIR and XPS spectra. The introduced double bonds make the membrane suitable for the covalent attachment of PAA polymer. The PAA-Def-PVDF membrane shows pH responsive behavior for both the hydraulic permeability and solute retention. This porous medium offers less resistance to solvent transport, allowing for higher permeation rates at much lower operating pressures with less energy consumption comparing to traditional NF membrane. The PAA-Def-PVDF membrane was also utilized as a support to immobilize metal nanoparticles to remove toxic chlorinated compounds (such as, TCE) from water. Asymmetric membranes with a macroporous sponge-like structure were successfully prepared by the phase inversion method in both lab-scale and large-scale. The modified PVDF membrane shows high surface area, high porosity and higher yield of PAA functionalization compared to traditional microfiltration PVDF membrane. The ion-exchange capacity of Ca^{2+} is 3.2 mg/cm^2 (265.1 mg/g), which is 10 times higher than that reported in our previous publications. The PAA-SPVDF membrane can be used to remove heavy metal ions from water due to its good ion-exchange properties. These two modifications of PVDF can extend the development of functionalized membranes with advanced applications.

DOI: 10.1021/ie504149t
Ind. Eng. Chem. Res. 2015, 54, 4174−4182

AUTHOR INFORMATION

Corresponding Author

*E-mail: db@engr.uky.edu. Phone No.: 859-257-2794. Fax: 859-323-1929.

Notes

The authors declare no competing financial interest.

ACKNOWLEDGMENTS

This research was supported by National Institute of Environmental Health Sciences Superfund Research Program (NIEHS-SRP, Award Number P42ES007380) and by the NSF KY EPSCoR (NSF Award no. 1355438) program. The authors acknowledge Ultura Inc., Oceanside, CA, for the joint development of full-scale PVDF membranes.

REFERENCES

(1) Liu, F.; Hashim, N. A.; Liu, Y.; Abed, M. R. M.; Li, K. Progress in the production and modification of PVDF membranes. *J. Membr. Sci.* **2011**, *375*, 1−27.

(2) Kang, G.-d.; Cao, Y.-m. Application and modification of poly(vinylidene fluoride) (PVDF) membranes − A review. *J. Membr. Sci.* **2014**, *463*, 145−165.

(3) Qu, T.; Pan, K.; Li, L.; Liang, B.; Wang, L.; Cao, B. Influence of Ultrasonication Conditions on the Structure and Performance of Poly(vinylidene fluoride) Membranes Prepared by the Phase Inversion Method. *Ind. Eng. Chem. Res.* **2014**, *53*, 8228−8234.

(4) Cui, Z.; Drioli, E.; Lee, Y. M. Recent progress in fluoropolymers for membranes. *Prog. Polym. Sci.* **2014**, *39*, 164−198.

(5) Hester, J. F.; Mayes, A. M. Design and performance of foul-resistant poly(vinylidene fluoride) membranes prepared in a single-step by surface segregation. *J. Membr. Sci.* **2002**, *202*, 119−135.

(6) Rahbari-Sisakht, M.; Rana, D.; Matsuura, T.; Emadzadeh, D.; Padaki, M.; Ismail, A. F. Study on CO2 stripping from water through novel surface modified PVDF hollow fiber membrane contactor. *Chem. Eng. J.* **2014**, *246*, 306−310.

(7) Thomas, R.; Guillen-Burrieza, E.; Arafat, H. A. Pore structure control of PVDF membranes using a 2-stage coagulation bath phase inversion process for application in membrane distillation (MD). *J. Membr. Sci.* **2014**, *452*, 470−480.

(8) Lu, J.; Kim, S.-G.; Lee, S.; Oh, I.-K. A Biomimetic Actuator Based on an Ionic Networking Membrane of Poly(styrene-alt-maleimide)-Incorporated Poly(vinylidene fluoride). *Adv. Funct. Mater.* **2008**, *18*, 1290−1298.

(9) Mika, A. M.; Childs, R. F.; Dickson, J. M.; McCarry, B. E.; Gagnon, D. R. A new class of polyelectrolyte-filled microfiltration membranes with environmentally controlled porosity. *J. Membr. Sci.* **1995**, *108*, 37−56.

(10) Mika, A. M.; Childs, R. F.; Dickson, J. M. Chemical valves based on poly(4-vinylpyridine)-filled microporous membranes. *J. Membr. Sci.* **1999**, *153*, 45−56.

(11) Xiao, L.; Isner, A.; Waldrop, K.; Saad, A.; Takigawa, D.; Bhattacharyya, D. Development of bench and full-scale temperature and pH responsive functionalized PVDF membranes with tunable properties. *J. Membr. Sci.* **2014**, *457*, 39−49.

(12) Ishihara, K.; Kobayashi, M.; Ishimaru, N.; Shinohara, I. Glucose Induced Permeation Control of Insulin through a Complex Membrane Consisting of Immobilized Glucose Oxidase and a Poly(Amine). *Polym. J.* **1984**, *16*, 625−631.

(13) Ishihara, K.; Muramoto, N.; Shinohara, I. Controlled Release of Organic Substances Using Polymer Membrane with Responsive Function for Amino Compounds. *J. Appl. Polym. Sci.* **1984**, *29*, 211−217.

(14) Nunes, S. P.; Sforça, M. L.; Peinemann, K.-V. Dense hydrophilic composite membranes for ultrafiltration. *J. Membr. Sci.* **1995**, *106*, 49−56.

(15) Brink, L. E. S.; Elbers, S. J. G.; Robbertsen, T.; Both, P. The anti-fouling action of polymers preadsorbed on ultrafiltration and microfiltration membranes. *J. Membr. Sci.* **1993**, *76*, 281−291.

(16) Iwata, H.; Matsuda, T. Preparation and properties of novel environment-sensitive membranes prepared by graft polymerization onto a porous membrane. *J. Membr. Sci.* **1988**, *38*, 185−199.

(17) Akhtar, S.; Hawes, C.; Dudley, L.; Reed, I.; Stratford, P. Coatings reduce the fouling of microfiltration membranes. *J. Membr. Sci.* **1995**, *107*, 209−218.

(18) Ying, L.; Kang, E. T.; Neoh, K. G. Characterization of membranes prepared from blends of poly(acrylic acid)-graft-poly-(vinylidene fluoride) with poly(N-isopropylacrylamide) and their temperature- and pH-sensitive microfiltration. *J. Membr. Sci.* **2003**, *224*, 93−106.

(19) Munari, S.; Bottino, A.; Capannelli, G. Casting and performance of polyvinylidene fluoride based membranes. *J. Membr. Sci.* **1983**, *16*, 181−193.

(20) Xu, J.; Bhattacharyya, D. Fe/Pd Nanoparticle Immobilization in Microfiltration Membrane Pores: Synthesis, Characterization, and Application in the Dechlorination of Polychlorinated Biphenyls. *Ind. Eng. Chem. Res.* **2006**, *46*, 2348−2359.

(21) Lewis, S. R.; Datta, S.; Gui, M.; Coker, E. L.; Huggins, F. E.; Daunert, S.; Bachas, L.; Bhattacharyya, D. Reactive nanostructured membranes for water purification. *Proc. Natl. Acad. Sci. U. S. A.* **2011**, *108*, 8577−8582.

(22) Bhattacharyya, D. Functionalized membranes and environmental applications. *Clean Techn Environ. Policy* **2007**, *9*, 81−83.

(23) Ross, G. J.; Watts, J. F.; Hill, M. P.; Morrissey, P. Surface modification of poly(vinylidene fluoride) by alkaline treatment1. The degradation mechanism. *Polymer* **2000**, *41*, 1685−1696.

(24) Wootthikanokkhan, J.; Changsuwan, P. Dehydrofluorination of PVDF and Proton Conductivity of the Modified PVDF/Sulfonated SEBS Blend Membranes. *Journal of Metals, Materials and Minerals* **2008**, *18*, 57−62.

(25) Kise, H.; Ogata, H. Phase transfer catalysis in dehydrofluorination of poly(vinylidene fluoride) by aqueous sodium hydroxide solutions. *Journal of Polymer Science: Polymer Chemistry Edition* **1983**, *21*, 3443−3451.

(26) Owen, E. D.; Shah, M.; Twigg, M. V. Phase transfer catalysed degradation of poly(vinyl chloride). I: Product characterisation and handling. *Polym. Degrad. Stab.* **1996**, *51*, 151−158.

(27) Crowe, R.; Badyal, J. P. S. Surface modification of poly-(vinylidene difluoride)(PVDF) by LiOH. *J. Chem. Soc., Chem. Commun.* **1991**, 958−959.

(28) Bottino, A.; Camera-Roda, G.; Capannelli, G.; Munari, S. The formation of microporous polyvinylidene difluoride membranes by phase separation. *J. Membr. Sci.* **1991**, *57*, 1−20.

(29) Sun, A. C.; Kosar, W.; Zhang, Y.; Feng, X. A study of thermodynamics and kinetics pertinent to formation of PVDF membranes by phase inversion. *Desalination* **2013**, *309*, 156−164.

(30) Fontananova, E.; Jansen, J. C.; Cristiano, A.; Curcio, E.; Drioli, E. Effect of additives in the casting solution on the formation of PVDF membranes. *Desalination* **2006**, *192*, 190−197.

(31) Gu, M.; Zhang, J.; Wang, X.; Tao, H.; Ge, L. Formation of poly(vinylidene fluoride) (PVDF) membranes via thermally induced phase separation. *Desalination* **2006**, *192*, 160−167.

(32) Smuleac, V.; Bachas, L.; Bhattacharyya, D. Aqueous-phase synthesis of PAA in PVDF membrane pores for nanoparticle synthesis and dichlorobiphenyl degradation. *J. Membr. Sci.* **2010**, *346*, 310−317.

(33) Xu, J.; Bhattacharyya, D. Membrane-based bimetallic nanoparticles for environmental remediation: Synthesis and reactive properties. *Environ. Prog.* **2005**, *24*, 358−366.

(34) Xiao, L.; Isner, A. B.; Hilt, J. Z.; Bhattacharyya, D. Temperature responsive hydrogel with reactive nanoparticles. *J. Appl. Polym. Sci.* **2013**, *128*, 1804−1814.

(35) Song, L.; Zhang, Z.; Song, S.; Gao, Z. Preparation and Characterization of the Modified Polyvinylidene Fluoride (PVDF) Hollow Fibre Microfiltration Membrane. *J. Mater. Sci. Technol.* **2007**, *23*, 55−60.

DOI: 10.1021/ie504149t
Ind. Eng. Chem. Res. 2015, 54, 4174−4182

(36) Lewis, S. Solution phase and membrane immobilized iron-based free radical reactions: Fundamentals and applications for water treatment. Ph.D Dissertation, University of Kentucky, 2011.
(37) Xu, J. Synthesis and Reactivity of Membrane-supported Bimetallic Nanoparticles for PCB and Trichloroethylene Dechlorination. Ph.D Dissertation, University of Kentucky, 2007.
(38) Himstedt, H. H.; Du, H.; Marshall, K. M.; Wickramasinghe, S. R.; Qian, X. pH Responsive Nanofiltration Membranes for Sugar Separations. *Ind. Eng. Chem. Res.* **2013**, *52*, 9259−9269.
(39) Zhao, C.; Nie, S.; Tang, M.; Sun, S. Polymeric pH-sensitive membranes—A review. *Prog. Polym. Sci.* **2011**, *36*, 1499−1520.
(40) Hollman, A. M.; Bhattacharyya, D. Controlled Permeability and Ion Exclusion in Microporous Membranes Functionalized with Poly(l-glutamic acid). *Langmuir* **2002**, *18*, 5946−5952.
(41) Hollman, A. M.; Scherrer, N. T.; Cammers-Goodwin, A.; Bhattacharyya, D. Separation of dilute electrolytes in poly(amino acid) functionalized microporous membranes: model evaluation and experimental results. *J. Membr. Sci.* **2004**, *239*, 65−79.
(42) Abitoye, J. O.; Mukherjee, P.; Jones, K. Ion Implantation: Effect on Flux and Rejection Properties of NF Membranes. *Environ. Sci. Technol.* **2005**, *39*, 6487−6493.
(43) Song, J.; Li, X.-M.; Figoli, A.; Huang, H.; Pan, C.; He, T.; Jiang, B. Composite hollow fiber nanofiltration membranes for recovery of glyphosate from saline wastewater. *Water Res.* **2013**, *47*, 2065−2074.
(44) Matheson, L. J.; Tratnyek, P. G. Reductive Dehalogenation of Chlorinated Methanes by Iron Metal. *Environ. Sci. Technol.* **1994**, *28*, 2045−2053.
(45) Zhang, W.-x.; Wang, C.-B.; Lien, H.-L. Treatment of chlorinated organic contaminants with nanoscale bimetallic particles. *Catal. Today* **1998**, *40*, 387−395.
(46) Lien, H.-L.; Zhang, W.-x. Nanoscale iron particles for complete reduction of chlorinated ethenes. *Colloids Surf. Physicochem. Eng. Aspects* **2001**, *191*, 97−105.
(47) Wang, C.-B.; Zhang, W.-X. Synthesizing Nanoscale Iron Particles for Rapid and Complete Dechlorination of TCE and PCBs. *Environ. Sci. Technol.* **1997**, *31*, 2154−2156.
(48) He, F.; Zhao, D.; Liu, J.; Roberts, C. B. Stabilization of Fe−Pd Nanoparticles with Sodium Carboxymethyl Cellulose for Enhanced Transport and Dechlorination of Trichloroethylene in Soil and Groundwater. *Ind. Eng. Chem. Res.* **2006**, *46*, 29−34.
(49) Smuleac, V.; Varma, R.; Sikdar, S.; Bhattacharyya, D. Green Synthesis of Fe and Fe/Pd Bimetallic Nanoparticles in Membranes for Reductive Degradation of Chlorinated Organics. *J. Membr. Sci.* **2011**, *379*, 131−137.
(50) Mi, F.-L.; Shyu, S.-S.; Wu, Y.-B.; Lee, S.-T.; Shyong, J.-Y.; Huang, R.-N. Fabrication and characterization of a sponge-like asymmetric chitosan membrane as a wound dressing. *Biomaterials* **2001**, *22*, 165−173.
(51) Xu, J.; Bhattacharyya, D. Fe/Pd Nanoparticle Immobilization in Microfiltration Membrane Pores: Synthesis, Characterization, and Application in the Dechlorination of Polychlorinated Biphenyls. *Ind. Eng. Chem. Res.* **2006**, *46*, 2348−2359.

DOI: 10.1021/ie504149t
Ind. Eng. Chem. Res. 2015, 54, 4174−4182